2020 American Control Conference
Denver, CO, USA, July 1-3, 2020

Bilateral Teleoperation of Soft Robots under Piecewise Constant Curvature Hypothesis: An Experimental Investigation

Lasitha Weerakoon[1] and Nikhil Chopra[1]

Abstract— **The field of soft robotics has evinced considerable interest recently due to its importance in several practical applications. Teleoperation of a soft manipulator to do a multitude of tasks in a remote environment is one such promising application. The dexterity and conformity of a soft robot can be constructively utilized for enhanced motion planning and manipulability in cluttered environments. To that end, this paper investigates an adaptive task space bilateral teleoperation framework for soft robots with dynamic uncertainties assuming a non-redundant rigid master manipulator and a redundant soft slave manipulator under the piecewise constant curvature hypothesis. First, the dynamics of the soft robot are approximated as a rigid link manipulator with elastic joints using an existing augmented formulation in the literature. The task space adaptive bilateral teleoperation framework is then introduced based on this rigid-robot-like formulation. The null space velocity of the soft robot is also exploited to achieve sub-task objectives. Finally, the proposed control algorithms are experimentally investigated on a planar soft robot and the results are discussed pointing out the important observations.**

I. Introduction

Soft robotics has become an expanding research area in the field of robotics since the agility and compliance of these robots can be exploited to achieve highly dexterous manipulation capabilities in cluttered environments [1]. Over the past two decades numerous applications of soft robots have been identified, such as minimally invasive surgery, operations in underwater and space environments, and inspection operations.

Typically a soft body is an infinite dimensional dynamical system. Therefore, it is a challenging task to articulate the kinematics and dynamics of the soft robot, which are amenable for control theoretical formulations. However, several reduced order mathematical models have been proposed in the soft robotics research recently. The kinematics of soft robots have been studied extensively and the *Piecewise Constant Curvature* (PCC) formulation is a widely used model [2]. Dynamics models proposed for soft robots have been based on PCC formulation [3], [4], [5] and Cosserat rod theory [6] among others [7], [8], [9].

Although several works on control and motion planning of soft robots have been developed recently, bilateral teleoperation of soft robot systems has not been addressed adequately [10]. However, for rigid link robotic systems bilateral teleoperation frameworks have been extensively studied [11], [12], etc. For soft robots, considering a kinematics framework, a telerobotic system for telesurgery has been proposed in [13]. A task space teleoperation framework considering the dynamics for an extensible soft robot using feedback linearization has been proposed in [14], [15]. The authors also have utilized the null space velocity of the redundant slave robot to achieve singularity avoidance as a sub-task. A model based nonlinear control strategy was utilized to achieve asymptotic task space tracking between the master device and the soft robots [16]. However, all these works did not include any feedback from the slave robot to the master robot, and hence the robots were not controlled bilaterally. Furthermore, dynamic uncertainty was not considered in the aforementioned works on teleoperation of soft robots.

One approach to mitigate the uncertainty of the parameters is to utilize adaptive control techniques [17]. There have been several previous studies on adaptive control of soft robots. A model reference adaptive control for soft robots [18] has been used in an open-loop inverse dynamic feedforward controller to follow reference trajectories in the degree of curvature space. A model-based sliding mode controller has also been developed for curvature tracking [15], [19]. Additionally, there have been several works on kinematic adaptive control of soft robots [20]. A model-free controller for continuum robots based on an adaptive Kalman Filter for path tracking using only actuation pressures and tip position has also been developed [21].

In the current paper, it is considered that the master/ leader robot is a non-redundant rigid manipulator and the slave/follower robot is a redundant inextensible soft manipulator under the PCC hypothesis. First, we map the kinematics and the dynamics of the soft slave robot to an approximated rigid robot using an augmented formulation [4]. Then the bilateral teleoperation framework is introduced using classical control strategies developed for rigid robots.

To the best of our knowledge, we demonstrate for the first time that passivity based adaptive task space controllers [12] can be constructively utilized for **bilateral teleoperation** of a rigid master robot and a soft slave robot. Consequently, the need for exact knowledge of the master or the soft robot's parameters is obviated. Additionally, the null space velocity tracking is utilized to achieve sub-task goals such as conforming to degree of curvature limits in the soft robot. Finally, the performance of the proposed controllers is evaluated extensively via experimentation with a physical planar soft robot and the gleaned insights are discussed.

[1]Department of Mechanical Engineering, University of Maryland, College Park, MD 20742, USA {lasitha, nchopra}@umd.edu

978-1-5386-8266-1/$31.00 ©2020 AACC

The rest of the paper is organized as follows. The mathematical models for the soft slave robot and the rigid master robot are introduced in Section II. Then the bilateral teleoperation framework for the system is discussed in Section III. In Section IV the experimental setup and the results for the proposed bilateral teleoperation framework for the soft robotic system are detailed. Finally, the summary of the paper is presented in Section V.

II. Mathematical Model

A. The Soft Manipulator: Slave robot

The dynamics of the soft slave robot is formulated as a Lagrangian system through an approximated dynamically consistent *augmented formulation* using the methods introduced in [4]. The reader is referred to [4] for the complete derivation.

Under the PCC hypothesis, the soft robot is assumed to be composed of n segments and each segment is assumed to have a constant curvature (CC) that is time dependent. To constitute the soft robot, these n CC segments are attached together in such a manner that the resulting curve is differentiable everywhere. Under this hypothesis a single variable per segment, namely the degree of curvature, is sufficient to describe the segment's configuration in space [2]. In this work, the segments are assumed to be inextensible.

The augmented robot model of this PCC robot is represented as a rigid link robot, as illustrated in Fig.1(a), with a sequence of revolute and prismatic (R and P) joints with elasticity. The *augmented formulation* approximates the kinematic and approximated dynamic properties of the PCC soft robot with a conventional rigid robot system. Under this formulation, the configuration variable of a segment is the degree of curvature q_{si}. Fig.1(b) illustrates a PCC robot comprised of three CC segments which also carries an end-effector approximated as a lumped mass at the end of the robot with mass m_e.

Following [4], the dynamics of the soft robot represented as an equivalent rigid robot evolving on the degree of curvature space $q_s \in R^n$ is given as,

$$M_s(q_s)\ddot{q_s} + C_s(q_s, \dot{q_s})\dot{q_s} + D\dot{q_s} + K_0 q_s + G_s(q_s) = \tau_s - J_s^\top(q_s)F_{ext} \quad (1)$$

where $M_s(q_s) \in R^{n\times n}$ is the equivalent inertial matrix, $C_s(q_s, \dot{q_s})\dot{q_s} \in R^n$ collects the equivalent centrifugal and Coriolis terms, $G_s(q_s) \in R^n$ is the equivalent gravitational torque and $\tau_s \in R^n$ is the generalized torque vector. Here, the damping and stiffness matrices, $D, K_0 \in R^{n\times n}$ respectively, are introduced to incorporate the compliance of the soft robot. $F_{ext} \in R^p$ is the external force acting on the end-effector which is mapped using the equivalent Jacobian $J_s(q_s) \in R^{p\times n}$.

B. The Rigid Manipulator : Master robot

The master robot is modeled as a rigid serial link manipulator with p links. In the absence of friction, the dynamics of the master robot can be written in the Euler-Lagrangian formulation as [22],

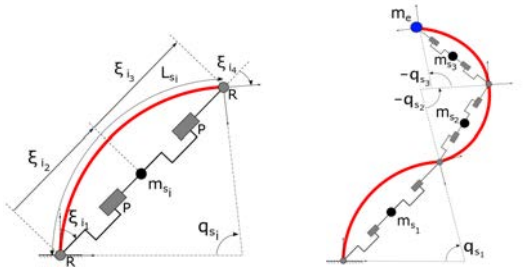

(a) (b)

Fig. 1. The PCC robot and the augmented robot as RPPR links are superimposed and shown here. The soft robot segments are shown in red. Panel (a) shows the i^{th} segment superimposed with RPPR model and panel (b) illustrates the representation of a soft robot manipulator with three CC segments with an end effector of lumped mass m_e at the tip.

$$M_m(q_m)\ddot{q}_m + C_m(q_m, \dot{q}_m)\dot{q}_m + G_m(q_m) = \tau_m + J_m^\top(q_m)F_h \quad (2)$$

where $M_m(q_m) \in R^{p\times p}$ is the inertial matrix, $C_m(q_m, \dot{q}_m)\dot{q}_m \in R^p$ is the matrix of the centrifugal and Coriolis terms and $G_m(q_m) \in R^p$ is the gravitational torque. Here,$q_m \in R^p$ is the vector of the relative joint angles, $\tau_m \in R^p$ is the control torque, and $F_h \in R^p$ is the operator force which is mapped using the Jacobian $J_m(q_m) \in R^{p\times p}$.

III. Bilateral Teleoperation Framework

The proposed bilateral teleoperation framework is developed based on the Lagrangian formulation of the soft slave robot and the rigid master robot as given by (1) and (2) assuming the master is non-redundant and the slave is redundant. We follow similar methods as in [12] to derive the framework. Subscripts $j = m, s$ will be used for concise representation where, subscript m refers to the rigid master robot and subscript s refers to the soft slave robot and the arguments will be omitted due to brevity, where obvious.

Consider the maps $h_m(\cdot) : R^p \to R^p$ and $h_s(\cdot) : R^n \to R^p$ which map the configuration spaces to the task space R^p. Here the direct forward kinematics of the robots are utilized as these maps and the robot tip positions and their velocities are defined as, $X_j = h_j(q_j)$ and $\dot{X}_j = J_j(q_j)\dot{q}_j$ respectively. Here, $J_j(q_j) = \frac{\partial h_j(q_j)}{\partial q_j}$ are the Jacobian matrices.

Following the passivity based adaptive control approach [17], assuming time invariant uncertainties in the inertia and Coriolis/centrifugal terms, the control inputs for the master and slave robots are given as,

$$\begin{aligned}\tau_m =& \hat{M}_m(q_m)a_m + \hat{C}_m(q_m, \dot{q_m})v_m + \hat{G}_m(q_m) \\ & - K_m s_m - J_m^T \bar{\tau}_m \\ \tau_s =& \hat{M}_s(q_s)a_s + (\hat{C}_s(q_s, \dot{q_s}) + \hat{D})v_s + \hat{K}_0 q_s + \hat{G}_s(q_s) \\ & - K_s s_s - J_s^T \bar{\tau}_s \end{aligned} \quad (3)$$

where $\hat{(\cdot)}$ indicates the estimates for the corresponding terms. K_j are positive definite diagonal matrices that needs to be tuned and $\bar{\tau}_j$ are the coordinating control torques that are defined subsequently.

Using the properties of Lagrangian systems we can define the regressor $(Y_i(q_i, \dot{q}_i, v_i, a_i))$ and parameter (Θ_i) vector pair for the estimated systems [22],

$$\hat{M}_m a_m + \hat{C}_m v_m + \hat{G}_m = Y_m \hat{\Theta}_m$$
$$\hat{M}_s a_s + (\hat{C}_s + \hat{D}) v_s + \hat{K}_0 q_s + \hat{G}_s = Y_s \hat{\Theta}_s \quad (4)$$

The tracking errors for the master system and soft slave system are defined as $e_m(t) = X_s(t - T_s) - X_m(t)$ and $e_s(t) = X_m(t - T_m) - X_s(t)$ respectively. Here, communication time delays T_s and T_m are assumed to be constant.

The signals $s_m(t)$ and $s_s(t)$ for the master the slave are defined as,

$$s_m = -J_m^{-1} \Lambda_m e_m + \dot{q}_m,$$
$$s_s = -J_s^{+} \Lambda_s e_s + \dot{q}_s - (I_n - J_s^{+} J_s)\psi_s \quad (5)$$

where Λ_j are positive definite matrices and $\psi_s \in R^p$ is the negative gradient of an appropriately defined convex function which is utilized for the sub-task control. $J_s^{+} \triangleq J_s^T (J_s J_s^T)^{-1} \in R^{n \times p}$ is the pseudo inverse of J_s and satisfies the property $J_s J_s^{+} = I_p$. The signals $v_i(t), a_i(t)$ are then defined as, $v_i = \dot{q}_i - s_i$ and $a_i = \ddot{q}_i - \dot{s}_i$, respectively.

The coordinating controls $\bar{\tau}_j$ are defined as,

$$\bar{\tau}_j = k_{r_j}(-\Lambda_j e_j + \dot{X}_j) - k_{J_j} \dot{e}_j \quad (6)$$

where k_{r_j} and k_{J_j} are positive control parameters.

The closed loop dynamics of the system is found by substituting the proposed controls (3) in (1)-(2) and using (4),

$$M_s \dot{s}_s + C_s s_s + D s_s + K_s s_s = Y_s \tilde{\Theta}_s - J_s^T \bar{\tau}_s - J_s^T F_{ext}$$
$$M_m \dot{s}_m + C_m s_m + K_m s_m = Y_m \tilde{\Theta}_m - J_m^T \bar{\tau}_m + J_m^T F_h \quad (7)$$

where $\tilde{\Theta}_j = \hat{\Theta}_j - \Theta_j$. The adaptation law for the parameter estimation is defined as,

$$\dot{\hat{\Theta}}_m = -\Gamma_m Y_m^T s_m \quad , \qquad \dot{\hat{\Theta}}_s = -\Gamma_s Y_s^T s_s \quad (8)$$

where Γ_m and Γ_s are positive definite symmetric control parameter matrices that needs to be chosen.

First, we consider the free motion case when there is no human operator force on the master and there is no environmental force on the slave (i.e: $F_h = F_{ext} = 0$). Following the proof of Theorem 3.1 of [12], assuming that J_m is full rank and operated under free motion of the closed loop teleoperation system (6) – (8), the tip of the soft slave manipulator asymptotically tracks the tip position and velocity of the rigid master manipulator. i.e: $e_i, e_s \to 0$ and $\dot{e}_m, \dot{e}_s \to 0$ as $t \to \infty$.

Next, we consider the case when the human operator exerts a force on the master and/or the slave robot experiences environmental forces. Here it is assumed that both the human operator and the slave environment are passive with respect to the inputs $F_h(t)$, $F_{ext}(t)$ and outputs $r_m = J_m s_m$, $r_s = J_s s_s$. Hence, there exist constants k_h, $k_e \in R^+$ such that $-\int_0^t F_h^T(\sigma) r_m(\sigma) d\sigma \leqslant -k_h$ and $\int_0^t F_{ext}^T(\sigma) r_e(\sigma) d\sigma \leqslant -k_e$.

Similarly to the free motion, assuming that J_m is full rank and the human operator and the slave environment are passive with respect to the inputs $F_h(t)$, $F_{ext}(t)$ and outputs r_m, r_s it can be shown that the closed loop teleoperation system described by (6) – (8) will drive $e_i, e_s \to 0$ and $\dot{e}_m, \dot{e}_s \to 0$ as $t \to \infty$ [12].

A. Sub-task Control in Null Space

In this work, the soft slave manipulator is assumed to be redundant considering the degree of curvature space with regard to the task space. Thus, $null(J_s)$ has a minimum dimension of $n - p$ which can be exploited to accomplish sub-task control as the task space motion is unaffected by the link velocity in the null space. This is done by designing the auxiliary function $\psi_s(t)$ in (5) appropriately.

The sub-task error is defined as the null space velocity tracking error of the auxiliary function $\psi_s(t)$ [23], $e_N(t) = (I_n - J_s^{+} J_s)(\dot{q}_s - \psi_s(t))$. Hence, the auxiliary function $\psi_s(t)$ can be designed in such a way that taking the negative gradient of a convex function $f(q_s)$ whose minima leads to the desired configuration, $\psi_s = -\frac{\partial}{\partial q} f(q)$.

In this work we will consider the sub-task of conforming to degree of curvature limits. We define the convex function $f_{\text{lim}}(q_s) = \Pi_{i=1}^{n} \big((1 - \frac{q_{s_i}}{q_{si}^{max}})(\frac{q_{s_i}}{q_{s_i}^{min}} - 1) \big)$ where q_{s_i} is the curvature of the i^{th} CC segment with $i = 1, ..., n$. $q_{s_i}^{max}$ and $q_{s_i}^{min}$ denotes the maximum and minimum allowable degree of curvature of the i^{th} CC segment. The corresponding auxiliary function for the sub-task is then found using computing ψ_s.

A detailed discussion of the different sub-tasks that could be achieved in bilateral teleoperation have been presented in [12]. Singularity avoidance and obstacle avoidance for soft robotic teleoperation also could be done by utilizing the subtask control and will be addressed in our subsequent work.

IV. Experimental Investigation

In this section we present the experimental results demonstrating the performance of the proposed bilateral teleoperation framework. First the experimental setup is described. Subsequently, the experimental results are presented and discussed.

A. Experimental setup

The experimental setup shown in Fig.2 consists of a pneumatically actuated pleated type soft robot [24], OptiTrack motion capture system and two i7 16GM RAM Windows 10 laptops: one running the control algorithms on Matlab 2015 and the other simulating the rigid master robot. Experiments with a physical rigid master robot will be reported in the future.

1) The Soft Robot: The soft robot used in the experiments, as shown in Fig.3(a), comprises of three bi-directional pleated type segments ($n = 3$) which were fabricated following methods outlined in [24]. The robot was constrained to move on a horizontal table and ball transfers were used underneath near the segment joints to reduce friction.

Each segment has two *compartments* that are individually actuated pneumatically. The segments are assumed to deform with a constant strain under the applied pressure, thus, having a constant curvature. The *middle layer* of each segment (the joint between the two chambers) is inextensible due to the restrained material layer. The segment lengths along the inextensible middle

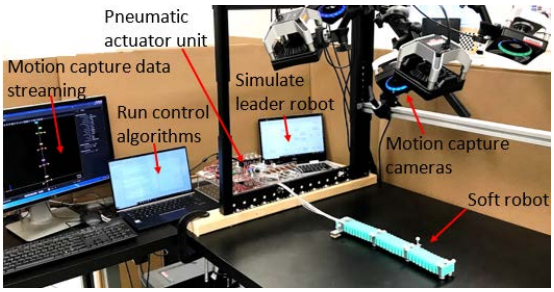

Fig. 2. The experimental setup.

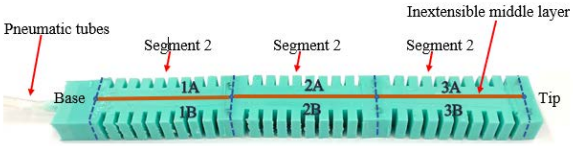

(a) Pleated type soft robot

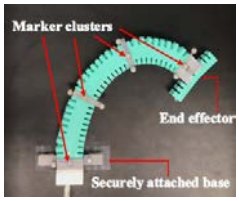

(b) Marker placement

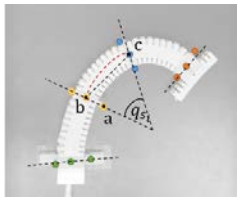

(c) Degree of curvature extraction

Fig. 3. Illustration of the soft robot and degree of curvature estimation using motion capture data of the markers.

layer were measured to be $L_{s_i} = 0.125$ m. The segment masses $m_{s_i} = 0.110$ kg were measured prior to joining the segments together. The material properties of each segment were assumed to be identical. Therefore, for all the segments identical torsional stiffness of $k_i = k$ and damping of $d_i = d$ were assumed. The identification of the nominal values of k and d will be discussed subsequently.

As seen in Fig.3(b), an unactuated end effector resembling a soft gripper of mass $m_e = 0.050$ kg was attached to the tip of the soft robot.

2) Degree of Curvature Estimation using Motion Capture: The positions of the end points of each segment was extracted using a Motion Capture system (OptiTrack) by attaching clusters of markers on the segment ends as shown in Fig.3(b). These labeled markers were assumed to be lying on the horizontal plane throughout the trial. The base of the soft robot was securely attached to the table so that experiments could be conducted without re-calibration. The degree of curvature of each segment was calculated using the properties of the dot product of the labeled marker positions as illustrated in Fig.3(c): $q_{s_i} = 2\left(\frac{\pi}{2} - \cos^{-1}\left(\frac{(a-b)\cdot(c-b)}{||a-b||\,||c-b||}\right)\right)$.

3) The Actuation Unit: The soft robot was actuated using a pneumatic controller unit based on the open source hardware platform [25] with command inputs serially transmitted to the control board. The compressed air to the unit was supplied by an external compressor at a constant pressure of 20psi. The air pressure in the segments was regulated by Pulse-Width Modulation (PWM) using a frequency of 100Hz. The control input calculated by the controller, in terms of a *torque*, was converted to a PWM signal for each segment using corresponding mappings. At a given time instance, only one compartment out of the two in each segment is actuated. A positive torque commanded one compartment while a negative torque commanded the opposite compartment of the same segment.

The torque-to-PWM signals mapping was identified by a curve fitting process for each compartment of the three segments. Considering the dynamic model of the soft robot (1), for the i^{th} segment, a step input of $\tau_{s_i} = \tau_{\text{pwm}}$ resulted in a steady state represented by $\tau_{i_{\text{pwm}}} = k\,\theta_{i_{\text{pwm}}}$. Here $\theta_{i_{\text{pwm}}}$ is the steady state degree of curvature of the considered i^{th} segment and k is the torsional stiffness. Sending commands to only one compartment of a segment, the steady state degree of curvatures ($\theta_{i_{\text{pwm}}}$) were recorded for different PWM signal values. Then the equivalent torque being applied, $\tau_{i_{\text{pwm}}}$, was calculated hypothesizing the torsional stiffness of each segment to be $k = 1$ Nm/rad. Finally, a third order polynomial curve fit was performed using this data for each of the segments to obtain the mapping from torque to PWM signal.

The nominal value of the torsional damping of a segment $d = 0.2$ Nms/rad was calculated using a system identification process by applying a unit torque to each of the segment.

B. Experimental results for bilateral teleoperation

Here we evaluate the performance of the passivity based task space adaptive bilateral teleoperation framework. In these experiments, the soft robot served as the slave device and a rigid manipulator which was simulated due to the unavailability of such a robot served as the master device. The simulation was done using Matlab/Simulink 2019a in real time using the Simulink Desktop Real-Time library block on a separate laptop. The communication between the two laptops, i.e. between the master and slave robots was achieved through the TCP/IP protocol over WiFi (network time delays: $T_m = T_s = 0.004s$).

The simulated master robot comprised of a 2-DoF rigid RR robot and was modeled according to [22]. The link lengths were chosen as $L_m = [0.1895, 0.1895]^\top$m so that the master robot and the soft slave robot has a similar task space. The masses and inertia were chosen as $m_m = [0.2, 0.2]^\top$kg and $I_m = [0.003, 0.003]^\top$kgm^2 respectively. The human force was modeled as spring-damper forces with spring and damper gains set to 150 N/m and 150 Ns/m respectively.

For the soft slave robot, the uncertainty was assumed in the segment masses, end effector mass, torsional stiffness and torsional damping. Thus the parameter vector was chosen as $\Theta_s = [m_{s_1}, m_{s_2}, m_{s_3}, m_e, k, d]^\top$ and the initial parameter estimates $\hat{\Theta}_s(0) = [0.5, 0.5, 0.5, 0.01, 2, 1]^\top$ were set different from the measured nominal values. The control gains were constant throughout the experiments and were set to $\Gamma_s = 0.075$, $\Lambda_s = 3.5$, $K_{rs} = K_s = 0.3$ and $K_{js} = 10$.

The uncertainty in the rigid master robot was assumed to be in the rigid robot's link masses and in the link inertia. Thus the parameter vector was chosen as $\Theta_m =$

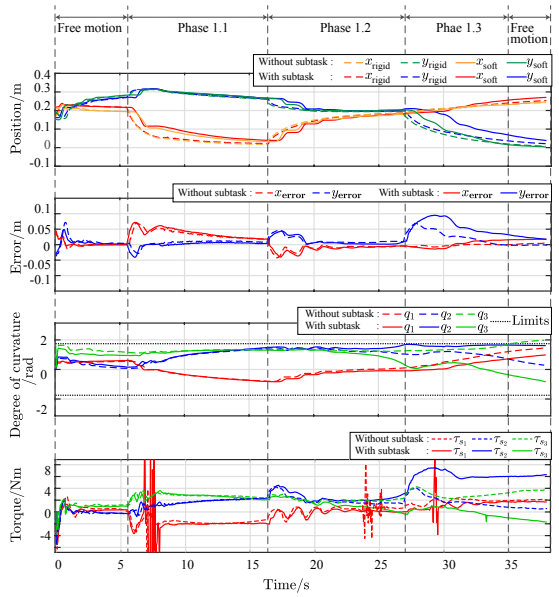

Fig. 4. Results for the bilateral teleoperation task without and with subtask control of conforming to degree of curvature limits for the scenario with no environmental force.

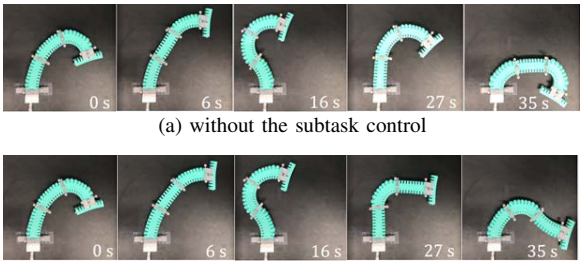

(a) without the subtask control

(b) with the subtask control

Fig. 5. Sequenced photographs of the bilateral teleoperation scenario with no environmental force.

$[m_{m_1}, m_{m_2}, I_{m_1}, I_{m_2}]^\top$. The initial parameter estimates were $\hat{\Theta}_m(0) = [0.05, 0.05, 0.001, 0.001]^\top$. The control gains were constant throughout the experiments and were set to $\Gamma_m = 0.75$, $\Lambda_m = 5$, $K_{rm} = K_m = 1$ and $K_{jm} = 12$.

1) Scenario with no environmental force: Here the soft slave robot was allowed to move freely with no environmental forces being applied. We considered the sub-task control of conforming to degree of curvature limits of $q_{s_i} = [\frac{-5\pi}{9}, \frac{5\pi}{9}]^\top$.

In the experiment, $t =$ 0-5.5s is in free motion for both the robots to synchronize. Then, from $t =$ 5.5-16.5s (phase 1.1) the human operator exerts a force to move the leader toward $X_m = [0.001, 0.245]^\top$. From $t =$ 16.5-27s (phase 1.2) the human operator tries to move the leader to $X_m = [0.2, 0.2]^\top$ and from $t =$ 27-35s (phase 1.3) to $X_m = [0.25, 0.001]^\top$. At $t =$ 35s the system is set to operate again in free motion.

Fig.4 illustrates the results of this scenario without and with the subtask control. Fig.5 depicts the configurations of the soft robot during the experiment. It is clearly seen from the sequenced photographs that the sub-task control forces the degree of curvatures of the segments to be within the desired limits by altering the configuration of the soft robot.

2) Scenario with the soft slave interacting with an obstacle: In this scenario an obstacle of the form of a wall

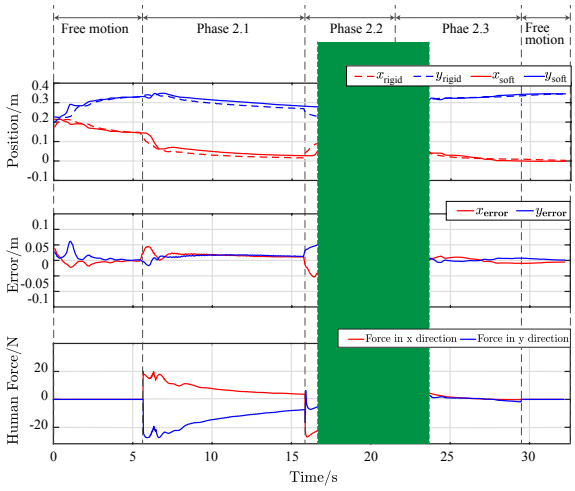

Fig. 6. The results of the bilateral operation involving obstacle contact in the slave environment. The forces experienced by the human is shown in the bottom plot.

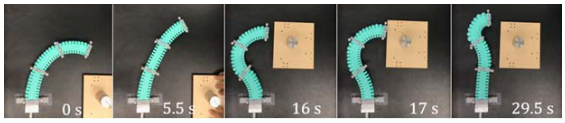

Fig. 7. Sequenced photographs of the bilateral teleoperation scenario with the soft slave interating with an obstacle

at $x = 0.05$ m appears during the trial at $t = 15$s and the trial was conducted without attaching an end effector.

In the initial 0 - 5.5s the robots operate in free motion. From $t =$ 5.5-15.5s (phase 2.1) the human operator moves the master toward $X_m = [0.001, 0.245]^\top$. From $t =$ 15.5-21.5s (phase 2.2) the human operator tries to move the master to $X_m = [0.2, 0.2]^\top$. The soft slave robot contacts the obstacle at around $t =$ 16.5s. Since the soft robot cannot move past the obstacle, the position errors between the two robot tips do not approach zero. Therefore, the human operator continuously tries to push toward the desired point despite the inability to move it any further. This is clearly illustrated in Fig.6 bottom figure showing that the environmental forces experienced by the soft robot at the slave environment are reflected onto the master side. From $t =$ 21.5-29.5s (phase 2.3) the human operator moves the master robot tip to the opposite direction of the obstacle, toward $X_m = [0.01, 0.33]^\top$. Now, it is observed that the tracking errors approach zero and the exerted forces diminish. At $t =$ 29.5s the system is set in free motion. Fig.6 presents the results of this trial and Fig.7 illustrates the configurations of the soft robot and the obstacle. The force feedback at the leader robot side is clearly seen in this experiment illustrating the performance of the proposed bilateral teleoperation framework.

C. Discussion

The goal of the experimental investigation was to study the performance of the proposed passivity based adaptive teleoperation framework for a pneumatically actuated soft robot. It should be noted that the reference trajectories and the target positions for all the trials were carefully considered in order for the soft robot to be able to operate in the task

space spanned by $q_{s_i} = [\frac{-5\pi}{9}, \frac{5\pi}{9}]^\top$ for all the segments so that the sub task control of conforming to degree of curvature limits of $q_{s_i} = [\frac{-5\pi}{9}, \frac{5\pi}{9}]^\top$ can be utilized.

In the experiments, although the results were satisfactory, the slow movement of the soft slave robot resulted in the slave robot not reaching the target reference positions in the allotted time interval. However, this observed result illustrates the critical need for bilateral teleoperation as the human operator is immersed in the remote slave environment and is able to respond to changes in the operational scenario.

The slow movement of the slave robot may be due to the *slow response* of the pneumatic actuation and also due to the *hysteresis effect* in the segments. Also spikes can be observed in the input where the large torques that are generated due to the *local singularities* of the segments.

Furthermore, although the stiffness of the segments were assumed to be constant, they may be changing with deformation. This time varying nature of the parameters are not handled by the passivity based adaptive control and it can impact the performance as well as the stability of the bilateral teleoperation system. The frictional effects were neglected in the soft robot model as well as in the control algorithms. However, there might have been a significant friction between the soft robot and the surface despite the addition of ball transfers.

V. Conclusion

This paper proposed an adaptive bilateral teleoperation framework for a system consisting of a non-redundant rigid master manipulator and a redundant PCC soft slave manipulator. The adaptive controllers guaranteed task space synchronization of the robots under time invariant parameter uncertainties at the master and/or soft slave side. The redundancy in the soft slave manipulator was exploited to achieve sub-task objectives such as conforming to curvature limits while tracking the position of the master robot. The experimental study demonstrated good task space tracking performance and immersion in the remote environment. Future work involves addressing practical limitations of the actuation mechanism as well challenges posed by the material properties.

VI. Acknowledgement

This research was supported in part by the National Science Foundation (NSF Grant No. ECCS1711554). The authors would like to thank the Robotics Realization Lab of the Maryland Robotic Center and the lab manager Dr.Ivan Pensky for helping to conduct physical experiments.

References

[1] T. George Thuruthel, Y. Ansari, E. Falotico, and C. Laschi, "Control strategies for soft robotic manipulators: A survey," *Soft robotics*, vol. 5, no. 2, pp. 149–163, 2018.

[2] I. Robert J. Webster and B. A. Jones, "Design and kinematic modeling of constant curvature continuum robots: A review," *The International Journal of Robotics Research*, vol. 29, no. 13, pp. 1661–1683, 2010.

[3] E. Tatlicioglu, I. D. Walker, and D. M. Dawson, "Dynamic modelling for planar extensible continuum robot manipulators," in *Proceedings 2007 IEEE International Conference on Robotics and Automation*. IEEE, 2007, pp. 1357–1362.

[4] C. Della Santina, R. K. Katzschmann, A. Bicchi, and D. Rus, "Model-based dynamic feedback control of a planar soft robot: trajectory tracking and interaction with the environment," *The International Journal of Robotics Research*, 2020.

[5] V. Falkenhahn, A. Hildebrandt, R. Neumann, and O. Sawodny, "Model-based feedforward position control of constant curvature continuum robots using feedback linearization," in *IEEE International Conference on Robotics and Automation*, 2015, pp. 762–767.

[6] F. Renda, F. Boyer, J. Dias, and L. Seneviratne, "Discrete cosserat approach for multi-section soft robots dynamics," *arXiv preprint arXiv:1702.03660*, 2017.

[7] S. H. Sadati, S. E. Naghibi, I. D. Walker, K. Althoefer, and T. Nanayakkara, "Control space reduction and real-time accurate modeling of continuum manipulators using ritz and ritz–galerkin methods," *IEEE Robotics and Automation Letters*, vol. 3, no. 1, pp. 328–335, 2017.

[8] G. S. Chirikjian, "Hyper-redundant manipulator dynamics: A continuum approximation," *Advanced Robotics*, vol. 9, no. 3, pp. 217–243, 1994.

[9] R. S. Penning and M. R. Zinn, "A combined modal-joint space control approach for continuum manipulators," *Advanced Robotics*, vol. 28, no. 16, pp. 1091–1108, 2014.

[10] C. G. Frazelle, A. D. Kapadia, K. E. Fry, and I. D. Walker, "Teleoperation mappings from rigid link robots to their extensible continuum counterparts," in *2016 IEEE International Conference on Robotics and Automation (ICRA)*. IEEE, 2016, pp. 4093–4100.

[11] Y. Dong and N. Chopra, "Passivity-based bilateral tele-driving system with parametric uncertainty and communication delays," *IEEE Control Systems Letters*, vol. 3, no. 2, pp. 350–355, 2018.

[12] Y.-C. Liu and N. Chopra, "Control of semi-autonomous teleoperation system with time delays," *Automatica*, vol. 49, no. 6, pp. 1553–1565, 2013.

[13] J. Burgner, D. C. Rucker, H. B. Gilbert, P. J. Swaney, P. T. Russell, K. D. Weaver, and R. J. Webster, "A telerobotic system for transnasal surgery," *IEEE/ASME Transactions on Mechatronics*, vol. 19, no. 3, pp. 996–1006, 2013.

[14] A. D. Kapadia, I. D. Walker, and E. Tatlicioglu, "Teleoperation control of a redundant continuum manipulator using a non-redundant rigid-link master," in *2012 IEEE/RSJ International Conference on Intelligent Robots and Systems*. IEEE, 2012, pp. 3105–3110.

[15] A. D. Kapadia, K. E. Fry, and I. D. Walker, "Empirical investigation of closed-loop control of extensible continuum manipulators," in *2014 IEEE/RSJ International Conference on Intelligent Robots and Systems*. IEEE, 2014, pp. 329–335.

[16] C. G. Frazelle, A. D. Kapadia, and I. D. Walker, "A nonlinear control strategy for extensible continuum robots," in *IEEE International Conference on Robotics and Automation*, 2018, pp. 7727–7734.

[17] J. . E. Slotine and L. Weiping, "Adaptive manipulator control: A case study," *IEEE Transactions on Automatic Control*, vol. 33, no. 11, pp. 995–1003, Nov 1988.

[18] E. H. Skorina, M. Luo, W. Tao, F. Chen, J. Fu, and C. D. Onal, "Adapting to flexibility: Model reference adaptive control of soft bending actuators," *IEEE Robotics and Automation Letters*, vol. 2, no. 2, pp. 964–970, April 2017.

[19] A. D. Kapadia, I. D. Walker, D. M. Dawson, and E. Tatlicioglu, "A model-based sliding mode controller for extensible continuum robots," in *Proceedings of the 9th WSEAS International Conference on Signal Processing, Robotics and Automation*, ser. ISPRA'10, Wisconsin, USA, 2010, pp. 113–120.

[20] H. Wang, B. Yang, Y. Liu, W. Chen, X. Liang, and R. Pfeifer, "Visual servoing of soft robot manipulator in constrained environments with an adaptive controller," *IEEE/ASME Transactions on Mechatronics*, vol. 22, no. 1, pp. 41–50, Feb 2017.

[21] M. Li, R. Kang, D. T. Branson, and J. S. Dai, "Model-free control for continuum robots based on an adaptive kalman filter," *IEEE/ASME Transactions on Mechatronics*, vol. 23, no. 1, pp. 286–297, Feb 2018.

[22] M. W. Spong, S. Hutchinson, M. Vidyasagar *et al.*, *Robot modeling and control*, 2006.

[23] P. Hsu, J. Mauser, and S. Sastry, "Dynamic control of redundant manipulators," *Journal of Robotic Systems*, vol. 6, no. 2, pp. 133–148, 1989.

[24] A. D. Marchese, R. K. Katzschmann, and D. Rus, "A recipe for soft fluidic elastomer robots," in *Soft robotics*, 2015.

[25] "Fluidic control board," last accessed on 03/16/2020. [Online]. Available: https://softroboticstoolkit.com/book/control-board